



저작자표시-비영리-변경금지 2.0 대한민국

이용자는 아래의 조건을 따르는 경우에 한하여 자유롭게

- 이 저작물을 복제, 배포, 전송, 전시, 공연 및 방송할 수 있습니다.

다음과 같은 조건을 따라야 합니다:



저작자표시. 귀하는 원저작자를 표시하여야 합니다.



비영리. 귀하는 이 저작물을 영리 목적으로 이용할 수 없습니다.



변경금지. 귀하는 이 저작물을 개작, 변형 또는 가공할 수 없습니다.

- 귀하는, 이 저작물의 재이용이나 배포의 경우, 이 저작물에 적용된 이용허락조건을 명확하게 나타내어야 합니다.
- 저작권자로부터 별도의 허가를 받으면 이러한 조건들은 적용되지 않습니다.

저작권법에 따른 이용자의 권리는 위의 내용에 의하여 영향을 받지 않습니다.

이것은 [이용허락규약\(Legal Code\)](#)을 이해하기 쉽게 요약한 것입니다.

[Disclaimer](#)

이학석사 학위논문

동중국해 과거 해양 표층 수온 프록시  
(알케논, 유공충의 Mg/Ca, 부유성 유공충  
군집, GDGT)

Past sea surface temperature proxies (alkenone, foraminiferal  
Mg/Ca, planktonic foraminiferal assemblage, GDGT) of the East  
China Sea



지도교수 이경은

2015년 8월

한국해양대학교 해양과학기술전문대학원

해양과학기술융합학과

김령아



이학석사 학위논문

동중국해 과거 해양 표층 수온 프록시  
(알케논, 유공충의 Mg/Ca, 부유성 유공충  
군집, GDGT)

Past sea surface temperature proxies (alkenone, foraminiferal  
Mg/Ca, planktonic foraminiferal assemblage, GDGT) of the East  
China Sea



지도교수 이경은

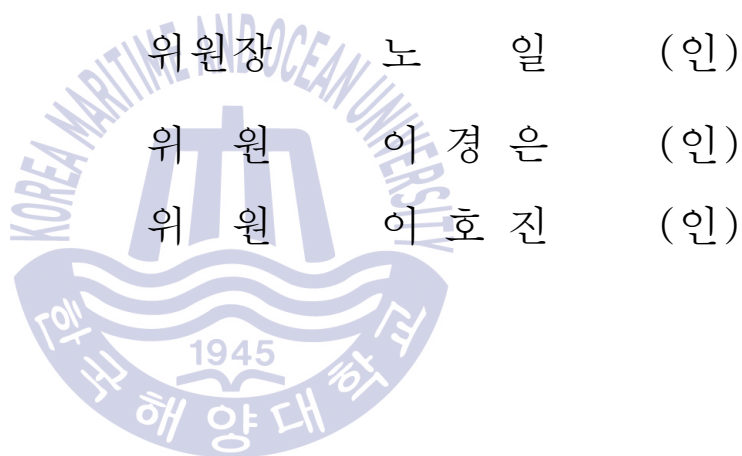
2015년 8월

한국해양대학교 해양과학기술전문대학원

해양과학기술융합학과

김령아

본 논문을 김령아의 이학석사 학위논문으로 인준함.



2015년 7월 14일

한국해양대학교 해양과학기술전문대학원

# Contents

List of Tables .....	iv
List of Figures .....	v
Abstract .....	viii
1. Introduction .....	1
2. Sediment cores	
2.1 Core stratigraphies .....	3
2.2 Chronology .....	6
2.3 Sedimentation rates .....	7
3. Temperatures from the SST proxies	
3.1 Alkenone based temperature .....	9
3.1.1 Habitat depth of alkenone producer .....	10
3.1.2 Alkenone seasonality .....	11
3.1.3 Comparison of core-top alkenone based temperatures with observed temperatures .....	13
3.2 Foraminiferal Mg/Ca ratio based temperature .....	14
3.2.1 Habitat depth of <i>G. ruber</i> .....	14
3.2.2 Seasonality of <i>G. ruber</i> .....	15
3.2.3 Comparison of core-top Mg/Ca ratio based temperatures with observed temperatures .....	15
3.3 Planktonic foraminiferal assemblage based temperature .....	17
3.3.1 Estimation techniques .....	18
3.3.2 Comparison of core-top planktonic foraminiferal assemblage based temperatures with observed temperatures .....	18

3.4 GDGTs based temperature .....	23
3.4.1 Habitat depth of GDGTs producer .....	23
3.4.2 Seasonality of GDGTs .....	24
3.4.3 Comparison of core-top GDGTs based temperature with observed temperatures .....	25
<b>4. Paleo-temperature estimates</b>	
4.1 Late Holocene (0 - 3 kyr) .....	26
4.2 Last Glacial Maximum (18 - 21 kyr) .....	29
4.3 Comparisons between SST proxies during the late Holocene and the LGM .....	30
<b>5. Uncertainties of calibration equations</b>	
5.1 Alkenone proxy .....	33
5.2 Foraminiferal Mg/Ca proxy .....	34
5.3 Planktonic foraminiferal assemblage proxy .....	34
<b>6. Conclusions</b> .....	37
<b>Acknowledgements</b> .....	39
<b>References</b> .....	40

## List of Tables

<b>Table 1</b> Marine sediment cores of the East China Sea used for past SST reconstruction .....	4
<b>Table 2</b> Methods and foraminiferal species used to date cores .....	6
<b>Table 3</b> Sedimentation rates of the Okinawa Trough during the late Holocene (0 – 3 kyr) and the LGM (18 – 21 kyr) .....	8
<b>Table 4</b> Comparison of errors in estimates of planktonic foraminiferal assemblage based temperatures calculated using four techniques. Calibration datasets used are also listed. References of each estimation error: MAT (Ortiz and MIX, 1997), RAM (Chen et al., 2005), SIMMAX-28 (Pflaumann and Jian, 1999), FP-12E (Thompson, 1981) .....	20



## List of Figures

- Fig. 1** Bathymetric map of the East China Sea. Black circles indicate the locations of sediment cores and blue triangles indicate the location of time-series sediment traps. Red squares indicate the location of water column studies. Dashed lines indicate the boundary dividing the Okinawa Trough into three regions (northern, middle and southern) ..... 3
- Fig. 2** Lithology of cores ..... 5
- Fig. 3** Sedimentation rates of cores collected from the northern (triangles), middle (circles) and southern (squares) Okinawa Trough ..... 7
- Fig. 4** Distribution of alkenone concentration in the water column and alkenone based temperatures reconstructed from suspended particulate organic matter at stations (a) 1 and (b) 8 (data from Nakanishi et al., 2012b). Observed temperatures in May (from JODC database) are also plotted ..... 10
- Fig. 5** Relative abundance of *Emiliania huxleyi* and *Gephyrocapsa oceanica* of time-series sediment traps at a station of SST2 (data from Tanaka, 2003). The traps deployed at water depth of (a) 600 m, (b) 800 m and (c) 1040 m ..... 12
- Fig. 6** Comparison of core-top alkenone based temperatures with observed temperatures at water depth of 0 - 30 m (from JODC database). (a) Cores KY07-04 PL-01 and MD982195, (b) Core DGKS9604 ..... 13
- Fig. 7** Seasonal variations in *Globigerinoides ruber* flux and relative abundance in a time-series sediment trap at station of JAST01 (data from Xu et al., 2005). The fluxes are plotted as bars; the relative abundance data are plotted as lines ..... 16
- Fig. 8** Seasonal variations in the *Globigerinoides ruber* flux in time-series sediment traps at station of SST2 (data from Yamasaki and Oda, 2003).

The traps deployed at water depth of (a) 606 m, (b) 813 m and (c) 1019 m ..... 16

**Fig. 9** Comparison of core-top Mg/Ca ratio based temperatures with observed temperatures at water depth of 0 – 50 m (from JODC database). (a) Core MD012403, (b) Core MD012404 and (c) Core KY07-04 PC-01 .... 17

**Fig. 10** Comparison of DGKS9603 core-top foraminiferal assemblage based summer and winter temperatures with observed SSTs (from JODC database). Core-top temperatures were reconstructed using MAT technique (Li et al., 2001) ..... 19

**Fig. 11** Comparison of MD012404 core-top foraminiferal assemblage based summer and winter temperatures with observed SSTs (from JODC database). Core-top temperatures were reconstructed using RAM technique (Chang et al., 2008) ..... 21

**Fig. 12** Comparison of 255 core-top foraminiferal assemblage based temperatures with observed SSTs (from JODC database). Core-top temperatures were reconstructed using FP-12E and SIMMAX-28 techniques (Jian et al., 2000) ..... 21

**Fig. 13** Comparison of B-3GC core-top foraminiferal assemblage based temperatures with observed SSTs (from JODC database). Core-top temperatures were reconstructed using FP-12E and SIMMAX-28 techniques (Jian et al., 2000) ..... 22

**Fig. 14** Distribution of GDGT concentration in the water column and GDGTs based temperatures reconstructed from suspended particulate organic matter at stations (a) 1 and (b) 8 (data from Nakanishi et al., 2012b). Observed temperatures in May (from JODC database) are also plotted ..... 24

**Fig. 15** Comparison of core-top GDGTs based temperature with observed SSTs (from JODC database) ..... 25

**Fig. 16** Paleo-temperatures reconstructed using different SST proxies in the Okinawa Trough. Triangles to the right of each graph indicate the 3 kyr averaged temperature. Numbers in parentheses indicate the corresponding observed temperature (from JODC database) ..... 27

**Fig. 17** (a) alkenone temperatures calculated using Müller et al. (1998); (b) alkenone temperatures calculated using Prah1 et al. (1988); (b) Differences between the two temperatures ..... 33

**Fig. 18** Comparison of foraminiferal assemblage based temperatures calculated using two different statistical techniques: FP-12E (a), SIMMAX-28 (b) and differences between them (c) ..... 35



# 동중국해 과거 해양 표층 수온 프록시 (알케논, 유공층의 Mg/Ca, 부유성 유공층 군집, GDGT)

Ryoung Ah Kim

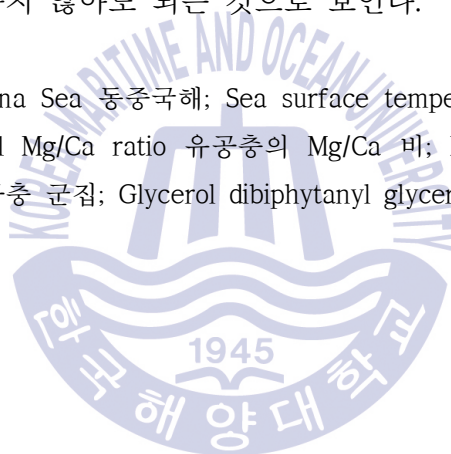
Department of Convergence Study on the Ocean Science and Technology  
Ocean Science and Technology School

## Abstract

동중국해 과거 표층 수온 복원에 사용된 알케논, *Globigerinoides ruber*의 Mg/Ca 비, 부유성 유공층 군집 그리고 glycerol dialkyl glycerol tetraether (GDGT) 프록시들을 비교하였다. 먼저 이러한 프록시로 복원된 온도들이 대표하는 온도를 알기 위해 수층에서 각 프록시와 관련된 생물들의 분포에 대해 조사하였다. 그리고 동중국해 해양 퇴적물로 복원된 프록시 온도들이 현재 표층 수온을 정확하게 반영하는지 확인하기 위해 최상부 퇴적물로 복원된 프록시 온도와 현재 표층 수온 (Japan Oceanographic Data Center, 1906 - 2003년 관측자료)을 비교하였다. 그 결과, 알케논 프록시로 계산된 온도는 연 평균 표층 수온을 대표하는 것으로 고려되며, 유공층의 Mg/Ca비 프록시로 계산된 온도는 여름 - 가을철 (6월 - 11월) 표층 수온을 대표하는 것으로 고려된다. 부유성 유공층 군집 프록시의 여름 표층 수온은 현재 여름 (8월) 표층 수온과 잘 일치하였지만, 겨울 표층 수온은 현재 겨울 (2월) 표층 수온보다  $\sim 3.6^{\circ}\text{C}$  더 높았다. 더 나아가 후기 홀로세 (0 - 3 kyr)와 마지막 최대

빙하기 (18 - 21 kyr)동안 복원된 온도들을 비교하였다. 부유성 유공충 군집으로부터 복원된 여름 표층 수온이 가장 높았고, 알케논으로 복원된 온도는 Mg/Ca 비로 복원된 온도보다 낮았다. 이는 아마도 유공충 군집의 여름 표층 수온이 8월 수온을 대표하고 알케논 온도와 Mg/Ca 온도는 각각 연 평균, 여름 - 가을 수온을 대표하기 때문일 것이다. 유공충 군집으로부터 복원된 겨울 표층 수온은 복원할 때 사용되는 통계학적 처리 방법이나 데이터베이스에 따라 온도가 다른 것으로 보인다. 반면, 알케논과 Mg/Ca 프록시는 실험 방법이나 계산식에 큰 영향을 받지 않았다. 따라서 동중국해 표층 수온 복원에는 알케논과 Mg/Ca 프록시가 적합한 것으로 생각된다. 이 때, 이들의 계절성을 고려해주어야 하며, 각 프록시가 대표하는 수심은 모두 혼합층 상부이므로 따로 구별하지 않아도 되는 것으로 보인다.

**KEY WORDS:** East China Sea 동중국해; Sea surface temperature 해양 표층 수온; Alkenone; Foraminiferal Mg/Ca ratio 유공충의 Mg/Ca 비; Planktonic foraminiferal assemblage 부유성 유공충 군집; Glycerol dibiphytanyl glycerol tetraether.



---

※ 이 석사학위논문에 게재된 상당수의 내용과 그림은 현재 국제전문학술지인 Progress in Earth and Planetary Science에서 심사 중 임.

## Chapter 1. Introduction

Past sea surface temperatures (SSTs) can be reconstructed from SST proxies including alkenone, glycerol dibiphytanyl glycerol tetraether (GDGT), planktonic foraminiferal Mg/Ca ratio, and planktonic foraminiferal assemblages. C<sub>37</sub> alkenone is known to be mainly produced by the haptophyte microalgae *Emiliania huxleyi*. Alkenone can be used to reconstruct SSTs because the degree of unsaturation of alkenone changes with seawater temperature (Brassell et al., 1986). Similarly, GDGT can be used as a proxy because the types of GDGTs produced by marine microbial *Crenarchaeota* change with seawater temperature (Schouten et al., 2002). The Mg/Ca ratio of planktonic foraminiferal calcite can also be used as a proxy for SST, because it changes with seawater temperature (Nurnberg et al., 1996). The planktonic foraminiferal assemblage technique is based on the compositional change in the foraminiferal assemblage with water temperature (Prell, 1985). Past February and August SSTs can be reconstructed from this proxy.

As the reconstruction of past SSTs from alkenone, Mg/Ca ratio and GDGT is based on the information recorded in marine organisms like coccolithophores, foraminifera and *Crenarchaeota*, knowledge on the habitat depth and seasonal abundance of these organisms is relevant. It is highly necessary to find out which depth and what season is accurately represented by the temperatures estimated using these proxies. A number of studies have reconstructed paleo SSTs using these proxies in the East China Sea (Jian et al., 2000; Li et al., 2001; Ijiri et al., 2005; Sun et al., 2005; Lin et al., 2006; Zhou et al., 2007; Chang et al., 2008; Yu et al., 2009; Chen et al., 2010; Kubota et al., 2010;

Nakanishi et al., 2012a). Some authors suggest that alkenone temperature might represent annual mean SST (Yu et al., 2009). However, other studies have suggested that alkenone temperature represents spring or spring-summer SSTs in the East China Sea (Ijiri et al., 2005; Zhou et al., 2007; Nakanishi et al., 2012a). *Globigerinoides ruber* Mg/Ca ratio temperature is thought to represent summer or warm period SSTs. The GDGT proxy has not been extensively studied in the East China Sea, and the representative depth of GDGT is unclear in this region (Nakanishi et al., 2012a). Thus, there is no consensus on what each proxy represents, and furthermore, no comparative assessment has previously been published regarding these proxies in the East China Sea.

Here we compared these four temperature proxies for reconstructing SSTs in the East China Sea. To find out what the proxy temperatures represent, we investigated the seasonal and vertical distribution pattern of each proxy-related producer in water column. In addition, we evaluated the planktonic foraminiferal assemblage technique. Furthermore, the proxy temperature estimates from core top sediments were compared with observed SSTs to confirm that proxy temperatures reconstructed from marine sediments can represent current SSTs in the East China Sea. Finally, we used the different proxies to reconstruct SSTs for the late Holocene (0 - 3 kyr) and the last glacial maximum (LGM) (18 - 21 kyr) and compared the reconstructed SSTs to evaluate the applicability of each proxy.

## Chapter 2. Sediment cores

### 2.1 Core stratigraphies

The sediment cores were recovered from the East China Sea (Fig. 1). Detailed information about core locations, water depth at the core sites are presented in Table 1. The sediment cores were mainly composed of homogeneous clay, silty clay, silt and clayey silt, except for core MD012404 (Jian et al., 2000; Li et al., 2001; Ijiri et al., 2005; Sun et al., 2005; Zhou et

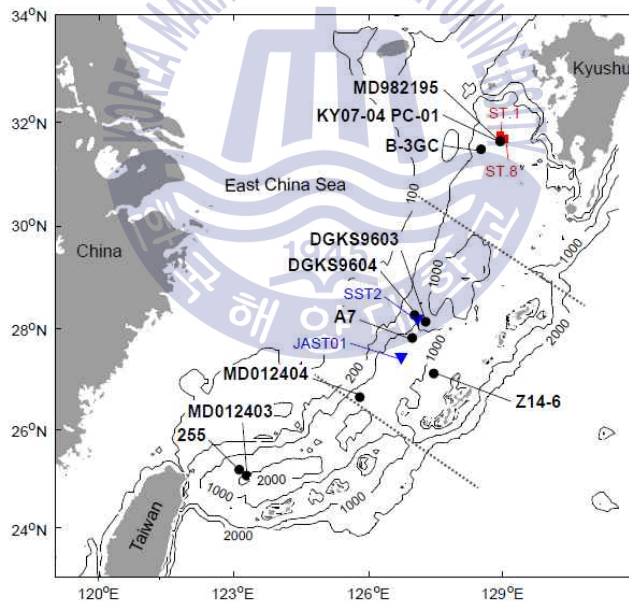


**Fig. 1** Bathymetric map of the East China Sea. Black circles indicate the locations of sediment cores and blue triangles indicate the location of time-series sediment traps. Red squares indicate the location of water column studies. Dashed lines indicate the boundary dividing the Okinawa Trough into three regions (northern, middle and southern).

al., 2007; Kao et al., 2008; Yu et al., 2009; Kubota et al., 2010) (Fig. 2). Core MD012404 was composed of nearly homogenous nannofossil ooze or diatom-bearing nannofossil ooze (Chang et al., 2009). Ash layers, including Kikai-Akahoya (K-Ah) and Aira-Tanzawa (AT), were found in cores A7, DGKS9603, KY07-04 PC-01 and MD982195. K-Ah and AT tephra likely come from the Kikai volcano (7.3 cal kyr B.P.) and the Aira volcano (26 – 29 cal kyr B.P.), respectively (Machida, 2002). There are some coarse-grained materials in cores MD012404 (pumice, volcanic glass), A7 (small turbidites) and MD982195 (sandy layer). <sup>14</sup>C dating results at the upper and lower limits of these coarse layers suggests that sedimentation was largely uninterrupted in these three cores (Ijiri et al., 2005; Sun et al., 2005, Fig. 2).

**Table 1** Marine sediment cores of the East China Sea used for past SST reconstruction.

Proxy	Core	Latitude	Longitude	Water depth (m)	Calibration equation	Reference
Alkenone	Z <sub>14-6</sub>	27° 07' N	127° 27' E	739	Müller et al. (1998)	Zhou et al. (2007)
	DGKS9604	28° 17' N	127° 01' E	766	Müller et al. (1998)	Yu et al. (2009)
	KY07-04 PC-01	31° 38' N	128° 57' E	758	Prahl et al. (1988)	Nakanishi et al. (2012a)
	MD982195	31° 38' N	128° 57' E	746	Prahl et al. (1988)	Ijiri et al. (2005)
Mg/Ca	MD012403	25.3° N	123.2° E	1420	Hastings et al. (2001)	Lin et al. (2006)
	MD012404	26° 39' N	125° 49' E	1397	Hastings et al. (2001)	Chen et al. (2010)
	A7	27° 49' N	126° 59' E	1264	Hastings et al. (2001)	Sun et al. (2005)
	KY07-04 PC-01	31° 38' N	128° 57' E	758	Hastings et al. (2001)	Kubota et al. (2010)
Foraminiferal assemblage	255	25° 12' N	123° 07' E	1575	FP-12E, SIMMAX28	Jian et al. (2000)
	MD012404	26° 39' N	125° 49' E	1397	RAM	Chang et al. (2008)
	DGKS9603	28° 09' N	127° 16' E	1100	MAT	Li et al. (2001)
	B-3GC	31° 29' N	128° 31' E	555	FP-12E, SIMMAX28	Jian et al. (2000)
GDGT	KY07-04 PC-01	31° 38' N	128° 57' E	758	Kim et al. (2010)	Nakanishi et al. (2012a)

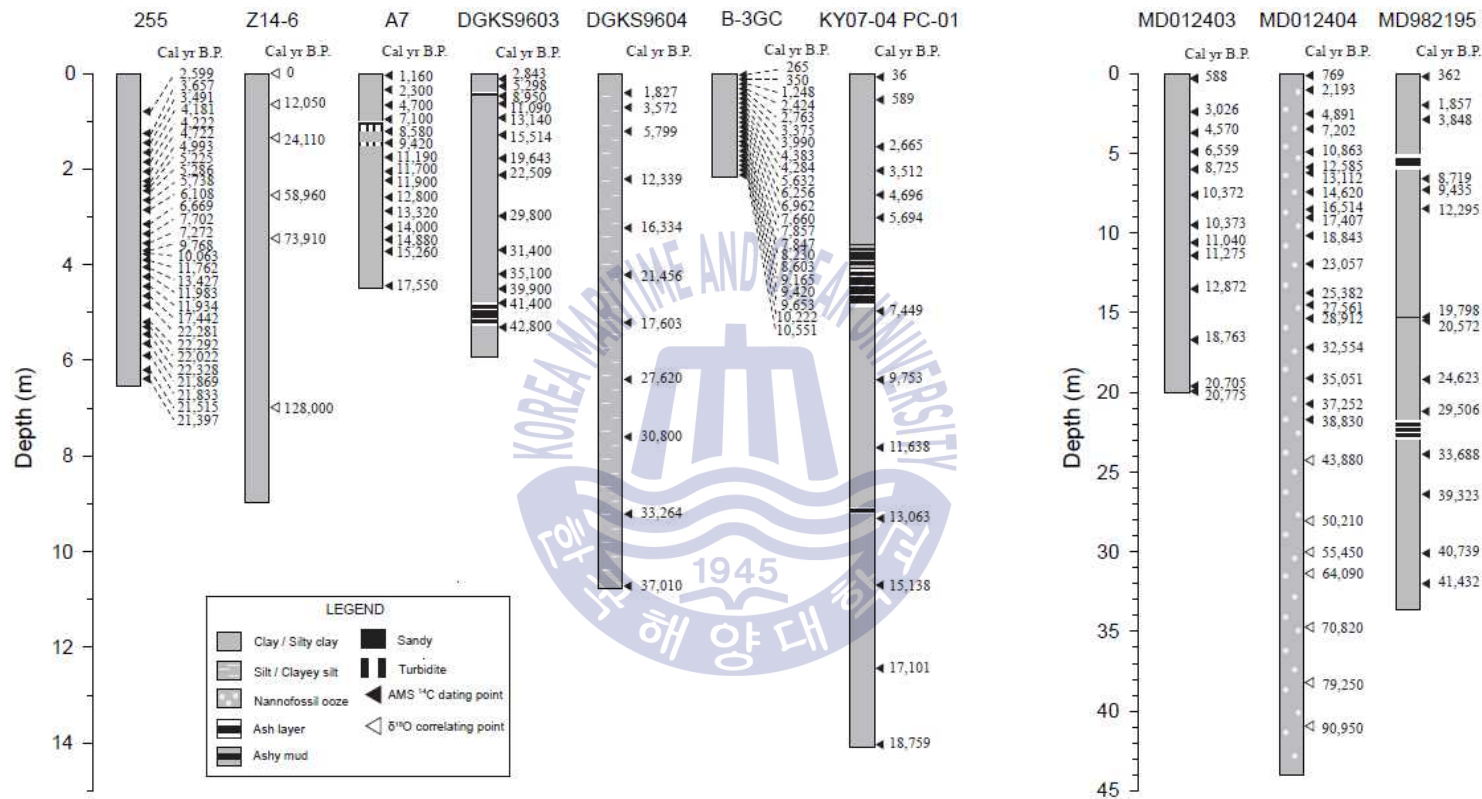


Fig. 2 Lithology of cores

## 2.2 Chronology

Ages of the cores were mainly determined based on radiocarbon dating of planktonic foraminifera (Table 2).  $^{14}\text{C}$  ages less than 20 kyr were converted to calendar ages using the CALIB program. The reservoir age for most of the cores was considered to be 400 yr. In core A7, however, a reservoir age of 700 yr was used because converted calendar ages were in good agreement with the K-Ah tephra age (Sun et al., 2005). Ages in core Z<sub>14-6</sub> were determined using the correlation between the cores' oxygen isotope curve and the  $\delta^{18}\text{O}$  stack curve (Zhou et al., 2007). Most of the cores have a sequential age. Age reversals between adjacent  $^{14}\text{C}$  dates were hardly found, except core 255 (Fig. 2). Due to non-sequential age, the part of core 255 older than 10 kyr BP was not used (Jian et al., 2000). Only two age reversals could be found in cores DGKS9604 and MD012403.

**Table 2** Methods and foraminiferal species used to date cores.

Core	method	Foraminiferal species	Reference
255	$^{14}\text{C}$	<i>Neogloboquadrina dutertrei</i>	Jian et al. (2000)
Z <sub>14-6</sub>	$\delta^{18}\text{O}$	<i>Globigerinoides sacculifer</i> , <i>Neogloboquadrina dutertrei</i>	Zhou et al. (2007)
A7	$^{14}\text{C}$	<i>Neogloboquadrina dutertrei</i>	Sun et al. (2005)
DGKS9603	$^{14}\text{C}$	<i>Globorotalia menardii</i> <i>Globigerinoides sacculifer</i> <i>Neogloboquadrina dutertrei</i>	Li et al. (2001)
DGKS9604	$^{14}\text{C}$	<i>Neogloboquadrina dutertrei</i> Planktonic foraminifer mixture at 1071 - 1074 cm	Yu et al. (2009)
B-3GC	$^{14}\text{C}$	<i>Neogloboquadrina dutertrei</i>	Jian et al. (2000)
KY07-04 PC-01	$^{14}\text{C}$	<i>Globigerina bulloides</i> <i>Neogloboquadrina dutertrei</i>	Kubota et al. (2010)
MD012403	$^{14}\text{C}$	Mixture of <i>Globigerinoides ruber</i> , <i>Globigerinoides sacculifer</i> , <i>Globigerinoides</i> <i>conglobatus</i> , <i>Globigerina quiquilateralis</i> and <i>Orbulina universa</i>	Kao et al. (2008)
MD012404	$^{14}\text{C}$	<i>Globigerinoides ruber</i> <i>Globigerinoides sacculifer</i>	Chang et al. (2009)
	$\delta^{18}\text{O}$	<i>Uvigerina spp.</i>	
MD982195	$^{14}\text{C}$	<i>Globigerina bulloides</i> <i>Neogloboquadrina dutertrei</i>	Ijiri et al. (2005)

## 2.3 Sedimentation rates

Sedimentation rates in the northern and southern parts of the Okinawa Trough in the East China Sea appear higher than those of the middle region (Fig. 3, Table 3). During the late Holocene, the sedimentation rates in the northern and southern regions are higher than about 50 cm/kyr, except for B-3GC core. Holocene sedimentation rates vary between 5 – 50 cm/kyr in the middle Okinawa Trough. During the LGM, sedimentation rates are either similar to or twice as high as sedimentation rates during the late Holocene (Table 3). Overall, sedimentation rates in the Okinawa Trough are high. So, the influence of bioturbation on the sedimentary records seems to be minimal. However, we cannot completely ignore the effect of bioturbation, because an age of 17,603 yr was measured between depths which had the ages of 21,456 yr and 27,620 yr in core DGKS9604 (Fig. 2).

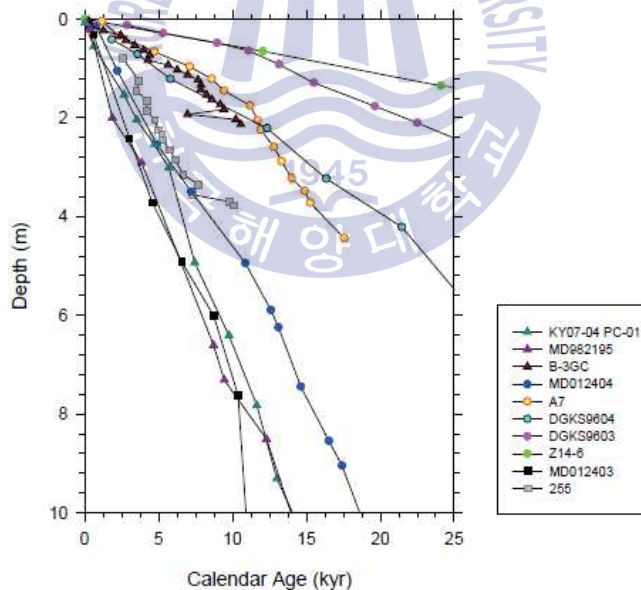
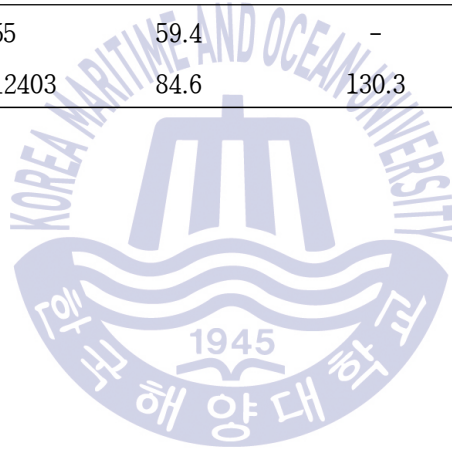


**Fig. 3** Sedimentation rates of cores collected from the northern (triangles), middle (circles) and southern (squares) Okinawa Trough.

**Table 3** Sedimentation rates of the Okinawa Trough during the late Holocene (0 – 3 kyr) and the LGM (18 – 21 kyr).

	Core	Sedimentation rate (cm/kyr)		Reference
		Late Holocene (0 – 3 kyr)	LGM (18 – 21 kyr)	
Northern Okinawa Trough	KY07-04 PC-01	55.3	102.0	Kubota et al. (2010)
	MD982195	66.1	74.2	Ijiri et al. (2005)
	B-3GC	10.3	-	Jian et al. (2000)
Middle Okinawa Trough	MD012404	53.6	52.4	Chang et al. (2009)
	Z <sub>14-6</sub>	5.4	5.8	Zhou et al. (2007)
	A7	18.2	31.4	Sun et al. (2005)
	DGKS9603	4.0	-	Li et al. (2001)
	DGKS9604	20.4	19.1	Yu et al. (2009)
Southern Okinawa Trough	255	59.4	-	Jian et al. (2000)
	MD012403	84.6	130.3	Kao et al. (2008)



## Chapter 3. Temperatures from the SST proxies

### 3.1 Alkenone based temperature

Alkenone unsaturation, which is quantified by geochemical analysis of marine sediments, can be converted into temperature using a calibration equation. According to Rosell-Melé et al. (2001), the alkenone-based temperature estimate remains largely unaffected by the method used. They suggest that alkenone-based temperature estimates are quite precise (margin of error:  $\pm 1.6^\circ\text{C}$ ). The alkenone unsaturation index is expressed by  $U^{K'}_{37}$  and can be calculated by following equation:

$$U^{K'}_{37} = [C_{37:2}] / ([C_{37:2}] + [C_{37:3}]) \quad (1)$$

$U^{K'}_{37}$  is converted to the alkenone temperature using one of two calibration equations: Prahl et al. (1988) (2) and/or Müller et al. (1998) (3):

$$T = (U^{K'}_{37} - 0.039) / 0.034 \quad (2)$$

$$T = (U^{K'}_{37} - 0.044) / 0.033 \quad (3)$$

The Prahl et al. (1988) equation (2) stems from an experimental culture of *Emiliania huxleyi*, which is an alkenone producer. The Müller et al. (1998) equation (3) is based on a comparison between core-top  $U^{K'}_{37}$  and annual mean sea surface (0m water depth) temperatures. These equations were used to reconstruct paleo-temperatures in the East China Sea in previous studies (Ijiri et al., 2005; Zhou et al., 2007; Yu et al., 2009; Nakanishi et al., 2012a, Table 1).

### 3.1.1 Habitat depth of alkenone producer

Although paleo-SSTs can be reconstructed using the alkenone unsaturation index (Brassell et al., 1986), alkenone-based temperatures do not always accurately represent SST, because of ambiguities concerning the habitat depth of alkenone producing species (Ohkouchi et al., 1999; Lee and Schneider, 2005). According to a study that compared alkenone-based temperatures calculated from surface sediments of the central Pacific Ocean with observed water column temperatures, alkenone temperatures in the mid-latitudes are consistent with thermocline temperatures (Ohkouchi et al., 1999). Another study also suggested that alkenone-based temperatures represent thermocline temperatures because alkenone concentrations were abundant at the subsurface in the water column of the central Pacific Ocean (Lee and Schneider, 2005). Nakanishi et al., (2012b) investigated the vertical distribution of alkenone concentrations at station 1 and station 8 in the East China Sea (Fig. 1 and 4). They showed that the alkenone concentration is 100 – 200

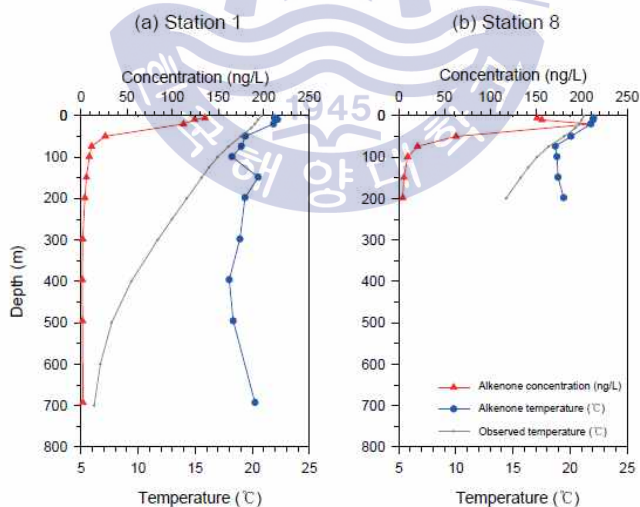


**Fig. 4** Distribution of alkenone concentration in the water column and alkenone based temperatures reconstructed from suspended particulate organic matter at stations (a) 1 and (b) 8 (data from Nakanishi et al., 2012b). Observed temperature in May (from JODC database) are also plotted.

ng/L at a depth of 0 – 25 m, whereas it is almost 0 ng/L at depths below 100 m. Moreover, alkenone-based temperatures reconstructed from suspended particulate organic matter were consistent with in situ shallow (above 100 m) water temperatures (Nakanishi et al., 2012b). Thus, they suggested that alkenone-based temperatures derived from alkenones preserved in sediments can be used to reconstruct SSTs in the East China Sea.

### 3.1.2 Alkenone seasonality

Ternois et al. (1996) suggested that seasonal variability in alkenone production should be considered if alkenones are used as proxies to reconstruct temperature. Some authors suggest that alkenone-based temperatures represent annual mean SSTs in the East China Sea (Yu et al., 2009). However, others suggest that alkenone-based temperatures may represent spring-summer SSTs in the East China Sea (Ijiri et al., 2005; Zhou et al., 2007). Tanaka (2003) investigated coccolith fluxes including *Emiliania huxleyi* and *Gephyrocapsa oceanica*, which are alkenone producer in time-series sediment traps installed in the Okinawa Trough from March 1993 until February 1994 (at station SST2, Fig. 1). In a sediment trap suspended close to the sea surface (Fig. 5a), the relative abundance of alkenone producers was about 70% of total coccolith flora during spring, but fell to less than 30% for the remaining period. However, in deep water sediment trap (installed 50 m above the bottom) (Fig. 5c), fluxes of alkenone producers remained constant and constituted about 60% of total coccolith flora in all seasons. Given this constant flux observed by Tanaka (2003) in deeper waters, alkenone temperatures reconstructed from sediments may represent the annual mean SST. According to another study on alkenones and alkyl alkenoates fluxes from time-series sediment traps installed in the northwestern Pacific

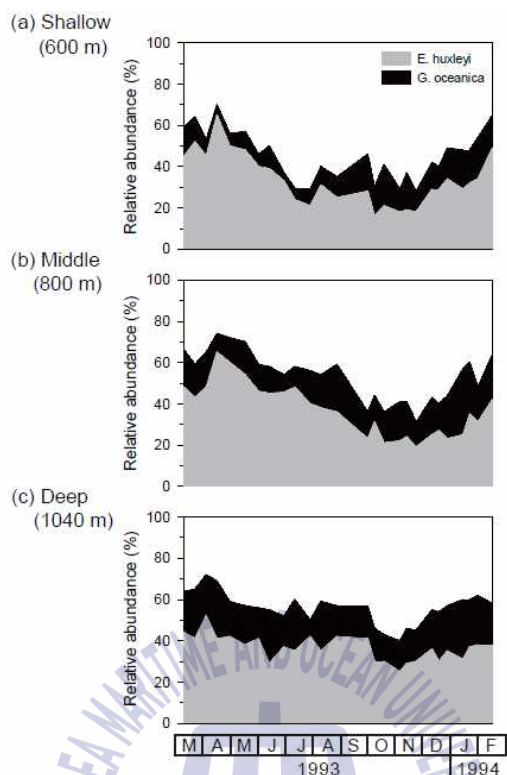


**Fig. 5** Relative abundance of *Emiliana huxleyi* and *Gephyrocapsa oceanica* of time-series sediment traps at a station of SST2 (data from Tanaka, 2003). The traps deployed at water depth of (a) 600 m, (b) 800 m and (c) 1040m.

Ocean from March 1991 until March 1992 (Sawada et al., 1998), there was no seasonality in alkenone flux in deep water. In a trap close to the surface, the fluxes were high (up to  $16.5 \mu\text{g}/\text{m}^2 \cdot \text{day}$ ) for the July - August period, but dropped to less than  $6 \mu\text{g}/\text{m}^2 \cdot \text{day}$  for the remaining experimental duration. However, in sediment traps suspended close to the bottom, fluxes remained constant (less than  $6 \mu\text{g}/\text{m}^2 \cdot \text{day}$ ) in all seasons. In addition, Sawada et al. (1998) compared the  $U^{K'}_{37}$  of core-top sediments with the  $U^{K'}_{37}$  of time-series sediment trap samples. The core-top  $U^{K'}_{37}$  is consistent with the flux-weighted annual mean  $U^{K'}_{37}$  of trap samples. Therefore, it seems that alkenone-based temperature represents annual mean temperature in the East China Sea.

### 3.1.3 Comparison of core-top alkenone based temperatures with observed temperatures

To examine whether the alkenone-based temperatures reconstructed from marine sediments represent SSTs, alkenone temperatures estimated using core top samples were compared with annual mean temperatures at water depths of 0 – 30 m (Fig. 6). The reason why the water depth was chosen is that a study on depth variation in alkenone concentration during spring bloom in 2008 shows that maximum concentration appears in the top 25 m (Nakanishi et al., 2012b). Annual mean temperatures were obtained from the Japan Oceanographic Data Center (JODC) (<http://www.jodc.go.jp>) (observed from 1906 to 2003). Core-top temperatures were calculated from sediments collected from the tops of cores KY07-04 PL-01, MD982195 and DGKS9604. There is no core-top sediment in core  $Z_{14-6}$ . Core KY07-04 PL-01 is a multiple core, which was recovered with core KY07-04 PC-01. Core-top sediment collected from the multiple core was used to reconstruct alkenone temperature because core-top sediment was missing in core KY07-04 PC-01 (Nakanishi et al.,

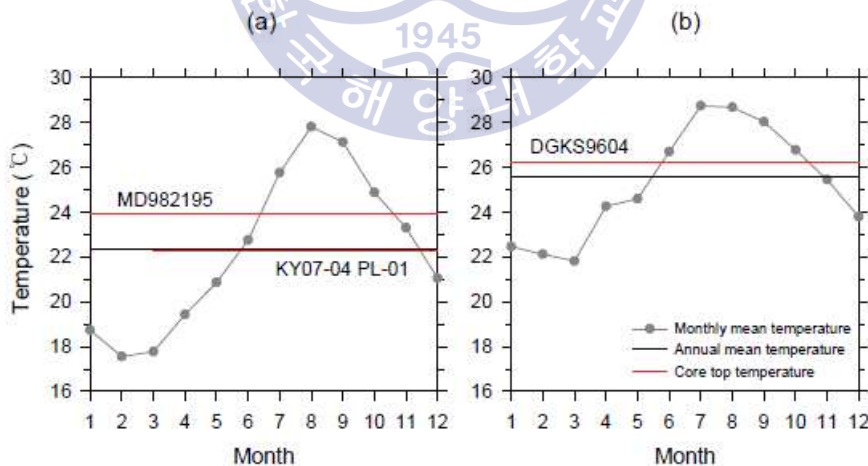


**Fig. 6** Comparison of core-top alkenone based temperatures with observed temperatures at water depth of 0 – 30 m (from JODC database). (a) Cores KY07-04 PL-01 and MD982195, (b) Core DGKS9604.

2012a). Annual mean temperatures of 22.3°C, 22.3°C and 25.6°C (at water column depths of 0 – 30 m, JODC data) corresponded with core-top alkenone temperatures of 22.3°C, 23.9°C and 26.2°C, calculated using cores KY07-04 PL-01, MD982195 and DGKS9604, respectively. Thus, temperatures reconstructed using core-top sediments were close to (less than 0.6°C different from) annual mean surface water temperatures at each location, except for core MD982195 (in which the core-top estimate is over one degree warmer). This suggests that the core-top sediment of core MD982195 might not be preserved well. However, based on the similarity with SSTs seen in data from the other two cores, we suggest that alkenone based temperatures reconstructed from core-top sediments can represent annual mean SST.

### 3.2 Foraminiferal Mg/Ca ratio based temperature

Many different calibration equations can be used to convert Mg/Ca ratios to SSTs (e.g. Nurnberg et al., 1996; Elderfield and Ganssen, 2000; Dekens et al., 2002; Anand et al., 2003). We chose the equation below (equation 4) because it was used previously to reconstruct SSTs in the East China Sea (Sun et al., 2005; Lin et al., 2006; Chen et al., 2010; Kubota et al., 2010). This equation was derived by Hastings et al. (2001) from studies that related core-top Mg/Ca ratios of *Globigerinoides ruber* with observed SSTs in the South China Sea:

$$T = \ln(\text{Mg/Ca} / 0.38) / 0.089 \quad (4)$$

#### 3.2.1 Habitat depth of *G. ruber*

Investigations of foraminiferal distribution in the Pacific, Atlantic and Indian oceans suggest that 75 – 100 % of *G. ruber* live at water depths of 0 – 40 m (van Donk, 1977). Furthermore, according to studies on oxygen isotope ratios of *G. ruber*, the habitat depth of *G. ruber* is 2 – 50 m in the South China Sea and 40 m in the region of southwest of Taiwan (Lin et al., 2004; Lin,

2014). Therefore Mg/Ca ratios of *G. ruber* are likely to record temperatures at depths of 0 – 50 m in the water column.

### 3.2.2 Seasonality of *G. ruber*

*G. ruber* is a tropical – subtropical species that is most abundant in warm waters (Bé and Tolderlund, 1971; Bijma et al., 1990). Hence the temperatures calculated using Mg/Ca ratios of *G. ruber* are thought to represent summer temperatures in the East China Sea (Sun et al., 2005; Lin et al., 2006; Chen et al., 2010; Kubota et al., 2010). Xu et al. (2005) examined *G. ruber* flux from time-series sediment traps installed in the middle region of the Okinawa Trough from October 1994 to August 1995 (at station JAST01, Fig. 1). According to this study, the relative abundance of *G. ruber* was 20% of total foraminiferal species during the summer – autumn period, but declined to 5% of total foraminiferal species in winter (Fig. 7). Yamasaki and Oda (2003) also examined *G. ruber* fluxes from time-series sediment traps installed in the mid region of the Okinawa Trough from March 1993 to February 1994 (at station SST2, Fig. 1). They found that *G. ruber* flux from summer – autumn was about three times more than that in winter, both at the sediment trap close to the surface as well as at the sediment trap close to the bottom (Fig. 8). Thus, we assumed that Mg/Ca temperatures of *G. ruber* represent summer – autumn temperatures in the East China Sea.

### 3.2.3 Comparison of core-top Mg/Ca ratio based temperatures with observed temperatures

To examine whether the Mg/Ca temperatures of marine sediments represent SSTs, core-top temperatures reconstructed using Mg/Ca ratios were compared with previously observed (JODC database) summer – autumn (June – November) mean water temperatures (depths of 0 – 50 m) (Fig. 9). The

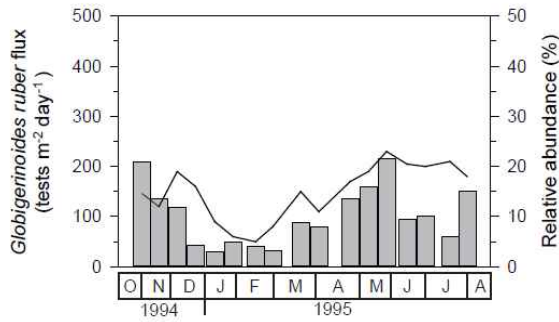


**Fig. 7** Seasonal variations in *Globigerinoides ruber* flux and relative abundance in a time-series sediment trap at station of JAST01 (data from Xu et al., 2005). The fluxes are plotted as bars; the relative abundance data are plotted as lines.

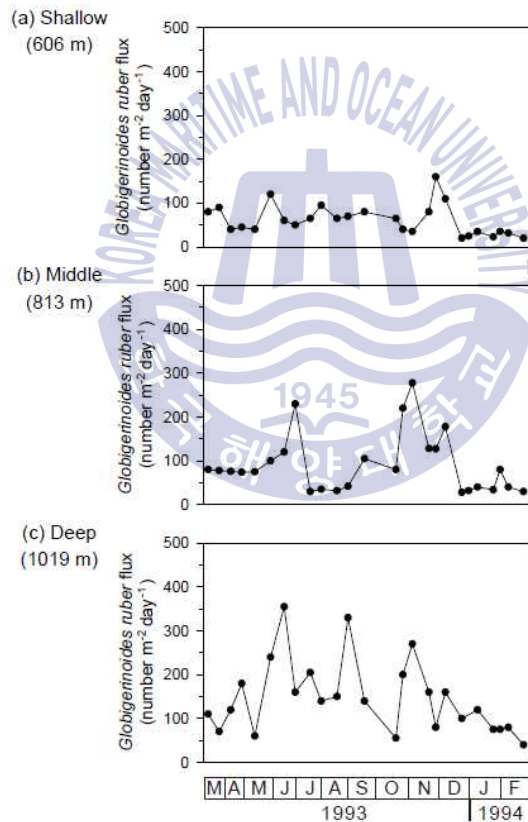


**Fig. 8** Seasonal variations in the *Globigerinoides ruber* flux in time-series sediment traps at station of SST2 (data from Yamasaki and Oda, 2003). The traps deployed at water depth of (a) 606 m, (b) 813 m and (c) 1019 m.

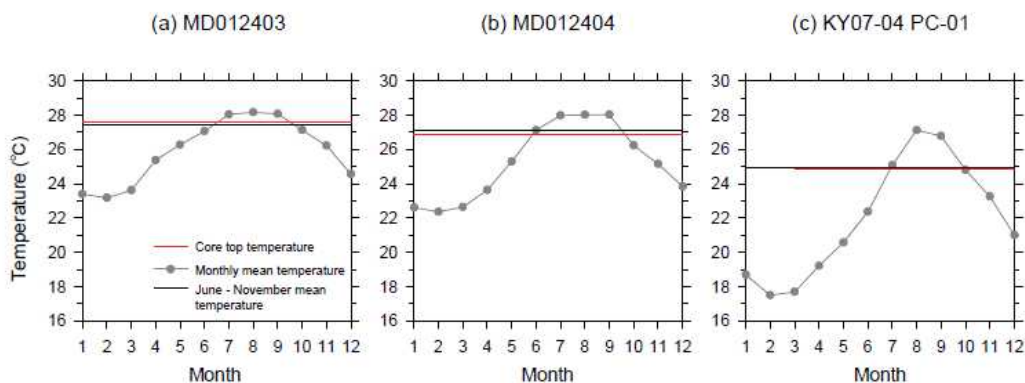


**Fig. 9** Comparison of core-top Mg/Ca ratio based temperatures with observed temperatures at water depth of 0 – 50 m (from JODC database). (a) Core MD012403, (b) Core MD012404 and (c) Core KY07-04 PC-01.

reason why the water depth was chosen is that habitat depth of *G. ruber* is considered to be in the range. Core-top Mg/Ca temperatures were reconstructed from cores MD012403, MD012404, and KY07-04 PC-01, from the southern, middle and northern parts of the Okinawa Trough in the East China Sea, respectively. Reconstructed core-top Mg/Ca temperatures of 27.6°C, 26.9°C and 24.9°C, closely mimicked observed mean temperatures of 27.5°C, 27.1°C and 24.9°C, respectively (June – November, water depths of 0 – 50 m, JODC database). Especially we examined seawater temperatures of 0 m, 0 – 30 m and 0 – 50 m from JODC database and found that the temperatures of the depths are almost identical to each other. Thus, we concluded that Mg/Ca ratios of *G. ruber* are consistent with summer – autumn SSTs in the East China Sea.

### 3.3 Planktonic foraminiferal assemblage based temperature

Data on planktonic foraminiferal assemblages can be converted into temperature estimates by statistical processing. Four statistical estimation techniques were used to reconstruct temperatures for the East China Sea

(Table 1).

### 3.3.1 Estimation techniques

Past February and August SSTs for the East China Sea were reconstructed from planktonic foraminiferal assemblage data by four estimation techniques: the modern analog technique (MAT), revised analog method (RAM), modern analog technique using a similarity method (SIMMAX-28) and FP-12E (Table 1). MAT uses a dissimilarity index to select core-top sediments that have foraminiferal assemblages similar to the foraminiferal assemblages of samples (Prell, 1985). The RAM technique is derived from the MAT technique. In this technique, the core-top sediments are selected based on a rate of increase in the dissimilarity index, using interpolated data on core-top fauna (from a database) (Waelbroeck et al., 1998). Waelbroeck et al. (1998) suggested that the RAM technique minimizes the uncertainty and biases of foraminiferal SST estimates. The SIMMAX technique uses a similarity index to select core-top sediments that have similar assemblage (Pflaumann et al., 1996). SIMMAX-28 was developed to reconstruct temperature in the western Pacific and is derived from the SIMMAX technique (Pflaumann and Jian, 1999). The FP-12E technique was developed from the Imbrie and Kipp transfer function method (IKM). It is appropriate for reconstructing the temperature of the northwestern Pacific region (Thompson, 1981). In the IKM technique, foraminiferal species are classified into several groups, which consist of foraminifera with similar characteristics, and SSTs are then estimated using a transfer function process (Imbrie and Kipp, 1971).

### 3.3.2 Comparison of core-top planktonic foraminiferal assemblage based temperatures with observed temperatures

To examine whether foraminiferal assemblage based temperatures of marine sediments are consistent with current SSTs, core-top summer and winter

assemblage temperatures were compared with observed temperatures in August and February (0 m, JODC database) (Fig. 10 - 13). Overall, as explained below, the accuracy of estimated temperature varied considerably depending on the statistical technique used to obtain the estimate.

Assemblage temperature of core DGKS9603 (middle Okinawa Trough) was reconstructed using the MAT technique (Li et al., 2001) (Fig. 10). Summer assemblage temperature of core-top sediment was 27.7°C, which was 1°C colder than the observed SST for August (29.0°C). Thus, foraminiferal summer temperature corresponded well with the observed August SST considering margin of error of  $\pm 1.50^\circ\text{C}$  (Ortiz and Mix, 1997) (Table 4). In contrast, the winter assemblage temperature of core-top sediment was 25.0°C, which was 3°C warmer than the observed February SST (22.1°C). Thus, assemblage winter temperature estimated using the MAT technique was not consistent with the observed February SST for this core considering the margin of error of  $\pm 1.50^\circ\text{C}$  (Ortiz and Mix, 1997).

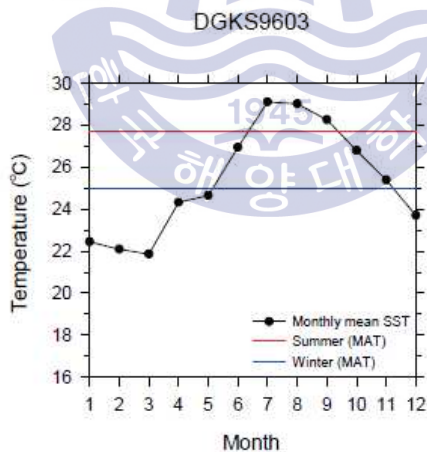


**Fig. 10** Comparison of DGKS9603 core-top foraminiferal assemblage based summer and winter temperatures with observed SSTs (from JODC database). Core-top temperatures were reconstructed using MAT technique (Li et al., 2001).

**Table 4** Comparison of errors in estimates of planktonic foraminiferal assemblage based temperatures calculated using four techniques. Calibration datasets used are also listed. References of each estimation error: MAT (Ortiz and MIX, 1997), RAM (Chen et al., 2005), SIMMAX-28 (Pflaumann and Jian, 1999), FP-12E (Thompson, 1981).

Method	Core	SST	Estimation error (°C)	Calibration dataset
MAT	DGKS9603	Summer Winter	$\pm 1.50$	Global
RAM	MD012404	Summer Winter	$\pm 0.72$ $\pm 1.17$	Western Pacific
SIMMAX-28	255 B-3GC	Summer Winter	$\pm 0.45$ $\pm 1.27$	Western Pacific
FP-12E	255 B-3GC	Summer Winter	$\pm 1.46$ $\pm 2.48$	North western Pacific

Summer and winter SSTs were reconstructed from core MD012404 (middle Okinawa Trough) using the RAM technique (Chang et al., 2008) (Fig. 11). Summer and winter assemblage temperatures of the core-top sediment were 28.6°C and 23.3°C, which were consistently close to (within the error range of  $\pm 0.72^\circ\text{C}$  for summer,  $\pm 1.17^\circ\text{C}$  for winter, Table 4) the respective observed SSTs for August (28.9°C) and February (22.5°C). Therefore, foraminiferal assemblage based temperatures estimated using the RAM technique from MD012404 core-top sediments represented observed SSTs.

Core 255 assemblage temperatures were reconstructed using both the FP-12E and SIMMAX-28 techniques (Jian et al., 2000) (Fig. 12). Foraminiferal summer core-top temperature estimates were 29.0°C (using FP-12E), and 28.8°C (using SIMMAX-28), both of which were consistent with the observed August SST (28.9°C). Foraminiferal winter temperatures were estimated at 24.3°C using both techniques (error of FP-12E:  $\pm 2.48^\circ\text{C}$ , error of SIMMAX-28:  $\pm 1.27^\circ\text{C}$ , Table 4). Considering the error, this estimated temperature was consistent with the observed February SST (23.3°C) for core 255 for both techniques.

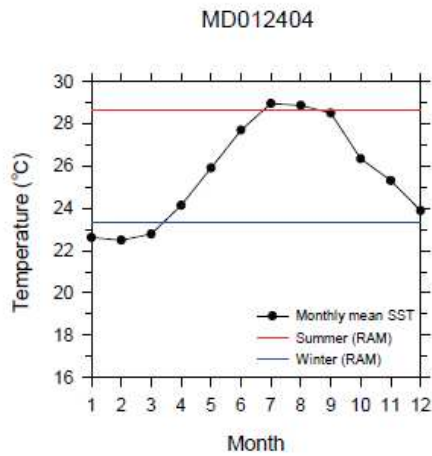


Fig. 11 Comparison of MD012404 core-top foraminiferal assemblage based summer and winter temperatures with observed SSTs (from JODC database). Core-top temperatures were reconstructed using RAM technique (Chang et al., 2008).

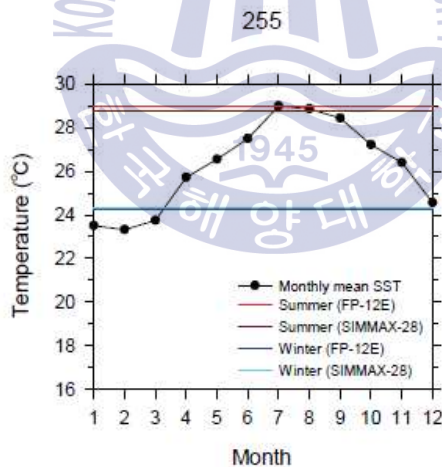
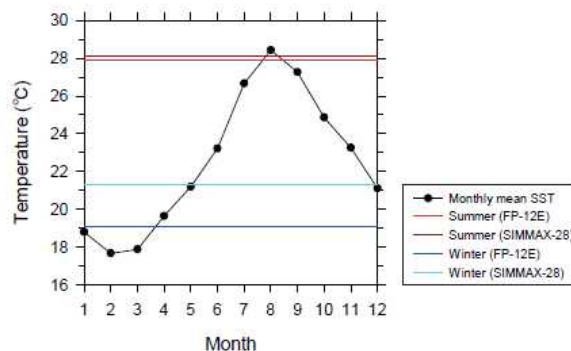


Fig. 12 Comparison of 255 core-top foraminiferal assemblage based temperatures with observed SSTs (from JODC database). Core-top temperatures were reconstructed using FP-12E and SIMMAX-28 techniques (Jian et al., 2000).

Core B-3GC assemblage temperatures were also reconstructed using both FP-12E and SIMMAX-28 techniques (Jian et al., 2000) (Fig. 13). Foraminiferal summer temperatures were found to be 27.9°C (FP-12E) and 28.1°C (SIMMAX-28), both of which were close to the observed August SST (28.4°C). Foraminiferal winter temperatures were 19.1°C (FP-12E) and 21.3°C (SIMMAX-28), whereas the observed February SST was 17.7°C. Considering the error ranges (FP-12E:  $\pm 2.48^\circ\text{C}$ , SIMMAX-28:  $\pm 1.27^\circ\text{C}$ , Table 4), the temperature estimated using the FP-12E technique is consistent with the observed February SST, but the temperature estimated using the SIMMAX-28 technique is not.

In summary, summer assemblage temperatures reconstructed from core-top sediments may represent the observed August SST. However, reconstructed winter assemblage temperatures may be somewhat higher than the observed February SST (Fig. 10 – 13). If these results may be expanded and assumed to apply to other cores, the RAM technique appears to be the most accurate statistical technique for estimating past August and February SSTs using the foraminiferal assemblage proxy for core-top sediments from the East China Sea.



**Fig. 13** Comparison of B-3GC core-top foraminiferal assemblage based temperatures with observed SSTs (from JODC database). Core-top temperatures were reconstructed using FP-12E and SIMMAX-28 techniques (Jian et al., 2000).

### 3.4 GDGTs based temperature

Change in GDGT with temperature can be expressed by the  $TEX_{86}$  index:

$$TEX_{86} = \frac{([GDGT-2] + [GDGT-3] + [Crenarchaeol regioisomer])}{([GDGT-1] + [GDGT-2] + [GDGT-3] + [Crenarchaeol regioisomer])} \quad (5)$$

A calibration equation converting  $TEX_{86}$  into temperature was suggested by Schouten et al. (2002). Since then, the calibration equation has been modified to improve estimation accuracy. In the East China Sea, GDGT temperatures were reconstructed using the  $TEX_{86}^H$  index (equation 6) and equation (7) (Kim et al., 2010):

$$TEX_{86}^H = \log (TEX_{86}) \quad (6)$$

$$T = 68.4 \text{ } TEX_{86}^H + 38.6 \quad (7)$$

#### 3.4.1 Habitat depth of GDGTs producer

The synthetic depth of GDGT is still controversial. Schouten et al. (2013) proposed that the depth of maximum GDGT abundance depended on regions. Nakanishi et al. (2012b) investigated the distribution of GDGTs and reconstructed GDGT temperatures from suspended particulate organic matter in the East China Sea (Fig. 1 and 14). They found that concentrations of GDGTs were constant throughout the water column (~5 ng/L). At depths of 100 – 200 m, GDGT based temperatures were consistent with in situ temperatures, but GDGT based temperatures at below 300 m were not consistent with GDGT based temperatures at depth of 100 – 200 m (Fig. 14a). Therefore, GDGT based temperature calculated from sediment samples is unclear.

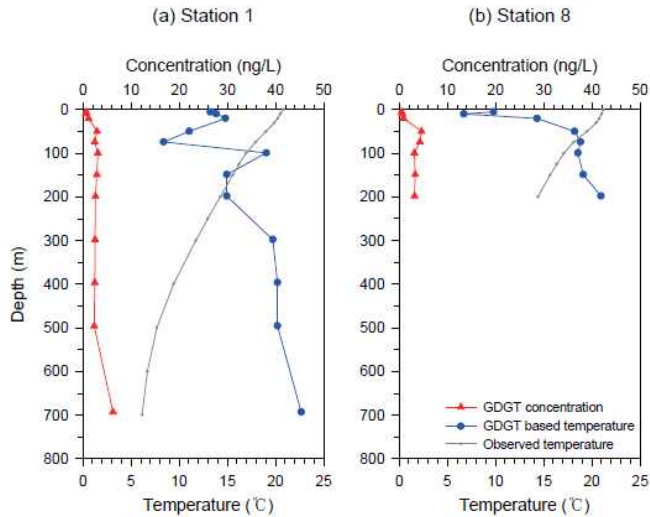


**Fig. 14** Distribution of GDGT concentration in the water column and GDGTs based temperatures reconstructed from suspended particulate organic matter at stations (a) 1 and (b) 8 (data from Nakanishi et al., 2012b). Observed temperatures in May (from JODC database) are also plotted.

### 3.4.2 Seasonality of GDGTs

The seasonality of GDGTs has been studied to improve biases inherent in GDGT based temperature estimates (reviewed by Schouten et al., 2013; Tierney, 2014). However, there is a lack of research on the seasonal variation of GDGTs from time-series sediment trap studies in the East China Sea. However, Yamamoto et al. (2012) examined GDGT flux in sinking particles using time-series sediment traps installed at three depths from November 1997 to August 1999 at a station in the northwestern Pacific. In the shallowest sediment trap, GDGT flux was higher than  $10 \mu\text{g}/\text{m}^2 \cdot \text{day}$  for the period from June 1998 to March 1999, but significantly lower for the remaining period. However, there was no seasonality in GDGT flux in deeper waters. Flux-weighted GDGT-based temperatures also corresponded roughly with mean annual SSTs. Therefore, GDGT-based temperature might represent the annual

mean surface temperature.

### 3.4.3 Comparison of core-top GDGTs based temperature with observed temperatures

To examine whether reconstructed GDGT-based temperatures of marine sediments are consistent with SSTs, core-top GDGT temperatures were compared with observed annual mean SSTs (JODC database) (Fig. 15). Kim et al. (2008) compared GDGT temperatures of the core-top sediments from a global dataset with observed temperatures recorded at water depths of 0 - 4000 m. They found that GDGT-based temperatures corresponded with annual mean surface water temperatures (0 m). So, we compared annual mean temperatures at 0 m depth (JODC database) with the core-top GDGT temperature of core KY07-04 PL-01. This core top temperature (22.6°C) was consistent with the observed temperature (22.6°C). However, due to the lack of specific studies on the habitat depth and seasonality of GDGTs in the water column of the East China Sea, we did not compare GDGT-based temperatures to paleo SSTs reconstructed for the late Holocene and LGM.

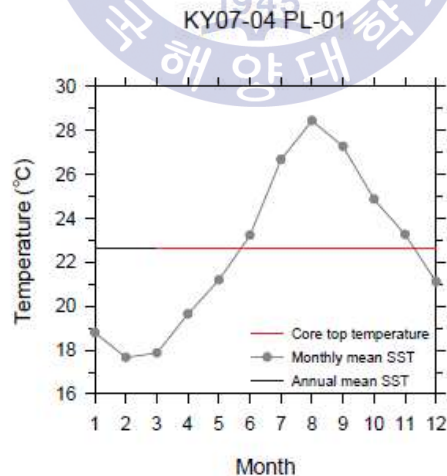


**Fig. 15** Comparison of core-top GDGTs based temperature with observed SSTs (from JODC database).

## Chapter 4. Paleo-temperature estimates

### 4.1 Late Holocene (0 - 3 kyr)

We compared observed current SSTs (JODC database) to 3 kyr averaged (late Holocene) paleo-temperatures reconstructed from marine sediments using alkenone, Mg/Ca ratio and foraminiferal assemblage proxies (Fig. 16a - 16c).

In the northern Okinawa Trough (Fig. 16a), reconstructed alkenone temperatures of cores KY07-04 PC-01 and MD982195 for the late Holocene were 23.8°C and 23.7°C, respectively. These paleo-temperature estimates are ~1.5°C warmer than the observed annual mean SST (22.3°C). According to a comparison of alkenone temperatures estimated from different 24 laboratories (Rosell-Melé et al., 2001), the precision of alkenone temperature estimates is about  $\pm 1.6^\circ\text{C}$  within 95% confidence level. We therefore suggest that reconstructed alkenone temperatures in the northern Okinawa Trough represent annual mean SSTs. In the middle Okinawa Trough (Fig. 16b), the 3 kyr averaged alkenone temperatures of cores Z<sub>14-6</sub> and DGKS9604 were 26.3°C and 26.1°C, respectively. These paleo-temperatures may appear to be about 1°C warmer than annual mean SSTs (25.0°C and 25.6°C, respectively), but given the margin of error of alkenone temperatures ( $\pm 1.6^\circ\text{C}$ ) (Rosell-Melé et al., 2001), they do in fact represent the annual mean SSTs.

Mg/Ca based temperature of core KY07-04 PC-01 (northern Okinawa Trough, Fig. 16a) during the late Holocene was 25.9°C, which, considering the margin of error ( $\pm 1 - 2^\circ\text{C}$ , Rosenthal et al., 2004), can represent observed June - November mean SSTs (24.9°C). Mg/Ca paleo-temperatures of cores

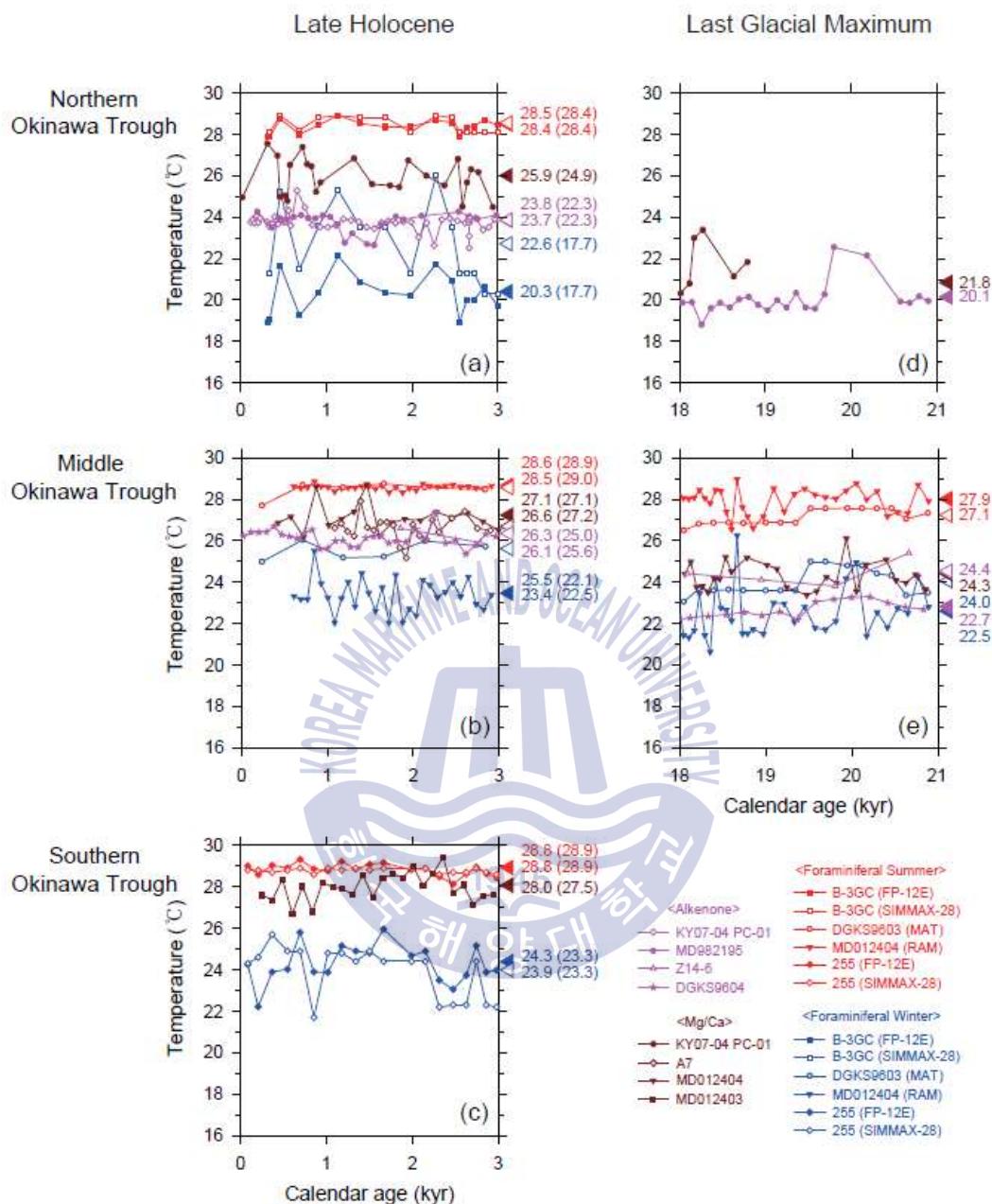


**Fig. 16** Paleo-temperatures reconstructed using different SST proxies in the Okinawa Trough. Triangles to the right of each graph indicate the 3 kyr averaged temperature. Numbers in parentheses indicate the corresponding observed temperature (from JODC database).

MD012404 and A7 (middle Okinawa Trough, Fig. 16b) were 27.1°C and 26.6°C, respectively, similar to the observed June – November mean SSTs (27.1°C and 27.2°C, respectively) when considering the margin of error for Mg/Ca temperature. In the southern Okinawa Trough (Fig. 16c), the Mg/Ca based paleo-temperature of MD012403 is 28.0°C, which can also represent the observed June – November mean temperature (27.5°C), given the margin of error.

Paleo summer SSTs obtained from the planktonic foraminiferal assemblage of core B-3GC (northern Okinawa Trough, Fig. 16a) were 28.5°C (SIMMAX-28) and 28.4°C (FP-12E). These paleo-temperatures are consistent with the observed August SST (28.4°C). In contrast, paleo winter assemblage temperatures are not consistent with the observed February SST. Paleo winter assemblage SSTs of core B-3GC core were 22.6°C (SIMMAX-28) and 20.3°C (FP-12E). Taking into account the error ranges of SIMMAX-28 ( $\pm 1.27^\circ\text{C}$ , Table 4) and FP-12E ( $\pm 2.48^\circ\text{C}$ , Table 4), winter assemblage SSTs are inconsistent with and 4.9°C and 2.6°C warmer, respectively, than the observed February SST (17.7°C).

Paleo summer assemblage SSTs of cores MD012404 and DGKS9603 (middle Okinawa Trough, Fig. 16b) were 28.6°C and 28.5°C, respectively. Considering the margin of error ( $\pm 0.72^\circ\text{C}$ ,  $\pm 1.50^\circ\text{C}$  respectively, Table 4), they are close to observed August SSTs (28.9°C and 29.0°C, respectively). In contrast, paleo winter assemblage SSTs are not consistent with February SSTs. The paleo winter assemblage temperature of MD012404 core is 23.4°C, which is consistent with the observed February SST (22.5°C) within the margin of error ( $\pm 1.17^\circ\text{C}$ , Table 4). However, overall, paleo winter SSTs are mostly warmer than the observed SSTs, as seen in cores from the middle Okinawa Trough. These results are consistent with our comparisons of observed SSTs with the winter assemblage SSTs of core-top sediments (in section 3.3.2).

The paleo summer assemblage SST of core 255 (southern Okinawa Trough,

Fig. 16c) was 28.8°C (this temperature estimate is the same whether the FP-12E or the SIMMAX-28 technique is used). The margins of error for the two techniques are:  $\pm 1.46^\circ\text{C}$  (FP-12E) and  $\pm 0.45^\circ\text{C}$  (SIMMAX-28), respectively (Table 4). Thus, paleo summer assemblage SST for core 255 corresponds well with the observed August SST (28.9°C). In contrast, winter assemblage SSTs are 24.3°C (FP-12E) and 23.9°C (SIMMAX-28), respectively, which are 1°C and 0.6°C warmer than February SST (23.3°C), considering the margin of error (FP-12E:  $\pm 2.48^\circ\text{C}$ , SIMMAX-28:  $\pm 1.27^\circ\text{C}$ , Table 4). Again, these paleo temperature comparisons are consistent with our previous results on assemblage based temperature estimates from core-top sediment SSTs (in section 3.3.2).

In summary, the SSTs reconstructed for the late Holocene from various proxies were compared with observed (present) SSTs (JODC database). During the late Holocene, the alkenone based temperature represents the present annual mean SST and the Mg/Ca based temperature represents the observed summer - autumn mean SST. In addition, assemblage based paleo summer SSTs were consistent with the observed August SST, but paleo assemblage based winter SSTs were usually higher than the present February SST. Then again, the winter SSTs deviated furthest from observed SSTs in the northern Okinawa Trough and paleo-temperature estimates based on assemblages gradually moved closer to observed SSTs with increasing southerly location of cores.

#### 4.2 Last Glacial Maximum (18 - 21 kyr)

We compared 3 kyr averaged temperatures reconstructed from alkenone, Mg/Ca and foraminiferal assemblage proxies during the late Holocene (0 - 3 kyr) with SSTs during the LGM (18 - 21 kyr), when the climate was dramatically different from the present (Fig. 16).

In the northern Okinawa Trough (Fig. 16a, 16d), alkenone based temperature

of core MD982195 was 20.1°C during the LGM, which was 3.6°C cooler than the late Holocene alkenone temperature. Although only 1000 yr of data exist for Mg/Ca based temperature for core KY07-04 PC-01 during the LGM, it appears to have been 4.1°C cooler during the LGM than during the late Holocene. Assemblage based temperatures could not be compared because there are no data during the LGM.

In the middle Okinawa Trough (Fig. 16b, 16e), alkenone based temperatures of cores Z<sub>14-6</sub> and DGKS9604 were 24.4°C and 22.7°C during the LGM, respectively, which are 1.9°C and 3.4°C colder than their respective alkenone temperatures during the late Holocene. The Mg/Ca temperature of core MD012404 is 24.3°C, which is 2.8°C colder than during the late Holocene. Summer assemblage SSTs of cores MD012404 and DGKS9603 were 27.9°C and 27.1°C, respectively, which are 0.7°C and 1.4°C colder than their respective late Holocene temperatures. Winter assemblage SSTs of cores MD012404 and DGKS9603 were 22.5°C and 24.0°C during the LGM, which are also 0.9°C and 1.4°C colder than during the late Holocene. There are no data on temperature proxies in the southern Okinawa Trough during the LGM.

Overall, comparisons of proxy temperatures between the two periods suggest that SSTs during the LGM were lower than during the late Holocene. However, the magnitudes of temperature differences are dependent on proxy. Alkenone and Mg/Ca based temperatures were 3 – 3.5°C lower during the LGM than in the late Holocene, whereas winter and summer assemblage SSTs decreased by only 1 – 1.2°C in the LGM (compared to the late Holocene).

### **4.3 Comparisons between SST proxies during the late Holocene and the LGM**

We compared the reconstructed SSTs between proxies in the Okinawa Trough. The middle Okinawa Trough was the region where most temperature data could be obtained from the three proxies used for paleo temperature

reconstructions (Fig. 16b, 16e).

First, alkenone temperatures were compared with Mg/Ca temperatures. Alkenone temperatures were lower ( $\sim 1^\circ\text{C}$ ) than Mg/Ca temperatures during the late Holocene. During the LGM, alkenone temperatures were still lower than Mg/Ca temperatures. It seems reasonable because alkenone temperature represents annual mean temperature, while Mg/Ca temperature represents summer - autumn temperature. At present annual mean temperature is lower than summer - autumn temperature in the area. In addition, water temperatures at surface are almost same to those at the range of 0 - 30 m and 0 - 50 m in the study area (JODC dataset, 1906-2003).

Second, Mg/Ca temperatures were compared with summer and winter assemblage temperatures. Since core-top and 3 kyr average winter temperatures of core DGKS9603 were about  $3^\circ\text{C}$  warmer than the present February SST, it was excluded from the comparison. During the late Holocene, Mg/Ca temperatures of cores A7 and MD012404 were  $26.6^\circ\text{C}$  and  $27.1^\circ\text{C}$ , respectively;  $1.5 - 2^\circ\text{C}$  colder than summer assemblage SSTs of MD012404 and DGKS9603 ( $28.6^\circ\text{C}$ ); and  $3.2 - 3.7^\circ\text{C}$  warmer than the winter SST of MD012404 ( $23.4^\circ\text{C}$ ). The lower Mg/Ca temperatures compared to summer assemblage based temperatures appear to be reasonable because Mg/Ca temperature represents summer - autumn temperature. During the LGM, the Mg/Ca temperature of MD012404 ( $24.3^\circ\text{C}$ ) was even colder than the summer assemblage SSTs of cores MD012404 and DGKS9603 ( $27.9^\circ\text{C}$  and  $27.1^\circ\text{C}$ , respectively). In contrast, the Mg/Ca temperature of MD012404 ( $24.3^\circ\text{C}$ ) is close to its winter SST ( $22.5^\circ\text{C}$ ), considering the margin of error ( $\pm 1 - 2^\circ\text{C}$ , Rosenthal et al., 2004).

Third, alkenone temperatures were compared with summer and winter assemblage SSTs. During the late Holocene, alkenone temperatures of cores Z<sub>14-6</sub> and DGKS9604 were  $26.3^\circ\text{C}$  and  $26.1^\circ\text{C}$ , respectively; about  $2.4^\circ\text{C}$  colder than summer assemblage SSTs of cores MD012404 and DGKS9603 (about 28.

6°C); and about 2.8°C warmer than the winter SST of core MD012404 (23.4°C). During the LGM, alkenone temperatures of cores Z<sub>14-6</sub> and DGKS9604 were 24.4°C and 22.7°C, respectively; about 3 - 5°C colder than their summer assemblage SSTs (27.9°C); but close to the winter assemblage SST of core MD012404 (22.5°C).

In summary, summer assemblage SSTs were the warmest among the three proxy SSTs during both the late Holocene and the LGM. Winter assemblage SSTs were lower than alkenone and Mg/Ca temperatures during the late Holocene, but close to these two other proxy temperatures during the LGM. It is possible that the warm winter assemblage SSTs are caused by the uncertainty in estimating foraminiferal assemblage based temperatures.



## Chapter 5. Uncertainties of calibration equations

### 5.1 Alkenone proxy

A comparison of the differences in alkenone temperature estimates obtained using the Prah1 et al. (1988) versus the Müller et al. (1998) calibration equations, for the East China Sea, suggests that temperatures calculated from Müller et al. (1998) equation are about 0.4 – 0.7°C warmer than SSTs calculated using the Prah1 et al. (1988) equation (Fig. 17). As this difference is

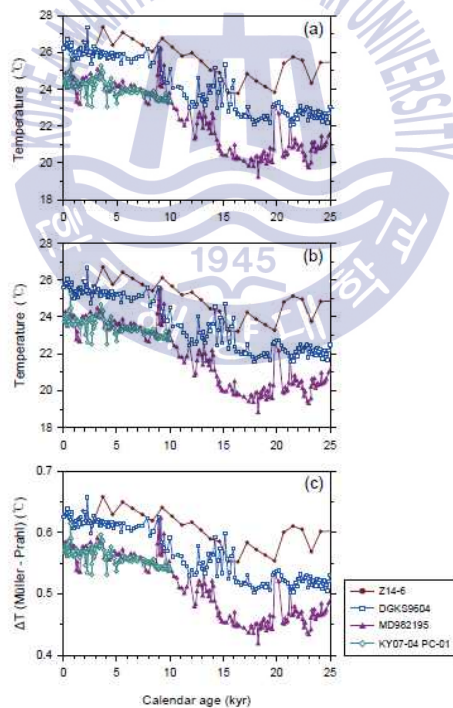


**Fig. 17** (a) alkenone temperatures calculated using Müller et al. (1998); (b) alkenone temperatures calculated using Prah1 et al. (1988); (c) Differences between the two temperatures.

much smaller than the precision of alkenone temperature estimates ( $\pm 1.6^\circ\text{C}$ ), alkenone temperatures do not differ significantly based on the calibration equation used.

## 5.2 Foraminiferal Mg/Ca proxy

Foraminiferal shells must be cleaned to remove clay minerals, organic matter and so on before samples can be geochemically analyzed to determine Mg/Ca ratios. Two cleaning methods (oxidative versus reductive protocols) may be used to clean shells. Some authors suggest that the Mg/Ca ratios of foraminifera are very sensitive to the cleaning method used (Barker et al. 2003). However, comparisons of Mg/Ca temperature reconstructed using *G. ruber* indicate that there is a difference of only about  $0.8^\circ\text{C}$  based on the cleaning protocol used (Kubota et al., 2010), which is within the margin of error ( $\pm 1 - 2^\circ\text{C}$ ). This suggests that cleaning method does not greatly influence Mg/Ca based temperature estimates. Furthermore, all Mg/Ca temperatures for the East China Sea were calculated using the Hastings et al. (2001) equation. So the question of error due to the use of a different equation does not arise.

## 5.3 Planktonic foraminiferal assemblage proxy

Core-top winter assemblage temperature estimates of core B-3GC differed depending on the statistical technique used for the estimation (Fig. 13). The temperature estimated using the FP-12E technique was consistent with February SSTs, but the temperature estimated using SIMMAX-28 was not. We examined the difference of temperatures estimated using FP-12E and SIMMAX-28 techniques (Fig. 18). The differences in summer temperatures (up to  $1^\circ\text{C}$ ) are larger than the error ranges for SIMMAX-28 ( $\pm 0.45^\circ\text{C}$ ), but not for FP-12E ( $\pm 1.46^\circ\text{C}$ ). Moreover, the differences in winter temperatures ( $3 - 4^\circ\text{C}$ ) are much larger than the error ranges for both methods:  $\pm 2.48^\circ\text{C}$

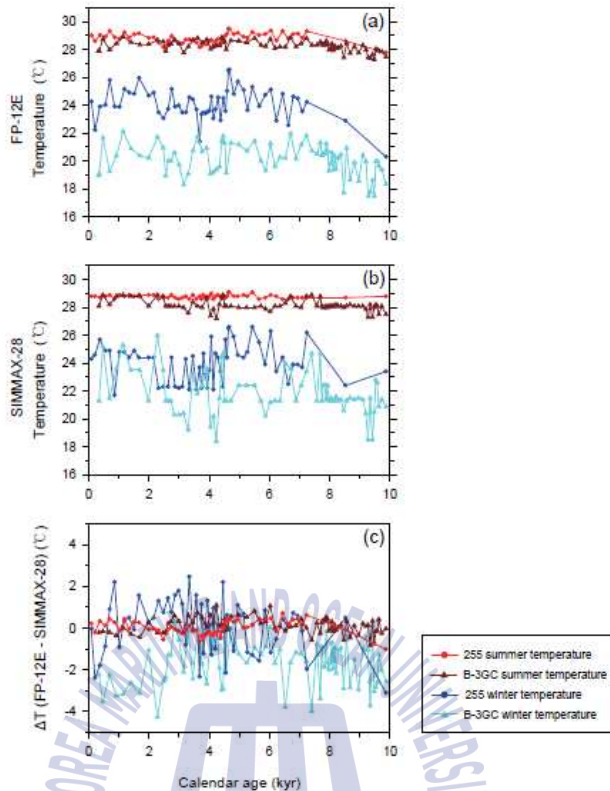


**Fig. 18** Comparison of foraminiferal assemblage based temperatures calculated using two different statistical techniques: FP-12E (a), SIMMAX-28 (b) and difference between them (c).

(FP-12E) and  $\pm 1.27^{\circ}\text{C}$  (SIMMAX-28). Therefore, temperatures estimated using the foraminiferal assemblage proxy seem to be influenced by statistical techniques.

Lee et al. (2010) used the MAT technique to reconstruct past SSTs of the East Sea for a global foraminiferal dataset, as well as for a regional dataset. MAT temperatures reconstructed using these two different foraminiferal assemblages (global dataset versus regional dataset) were completely different. We felt that in this case, temperature estimates obtained from the East Sea dataset were more reliable because it is difficult to find core-top sediments in the global dataset that have foraminiferal assemblages resembling those of the

East Sea. The western Pacific and northwestern Pacific datasets were used to reconstruct past SSTs for the East China Sea (Table 4) except for core DGKS9603 (global dataset). Core-top winter temperatures of core DGKS9603 were 3°C warmer than the observed February SST (Fig. 10). Moreover, average winter temperatures during the late Holocene (0 - 3 kyr) were also 3.4°C warmer than observed February SST (Fig. 16b). Furthermore, during the LGM, the average temperature is 2°C warmer than the observed February SST. Thus, foraminiferal assemblage based winter temperatures seem to be largely influenced by the dataset used.



## Chapter 6. Conclusions

As there are no studies on GDGT seasonality of the East China Sea, we decided to focus our discussion and analyses on the three other proxies we studied: alkenones, Mg/Ca ratios and planktonic foraminiferal assemblages.

Alkenones were most abundant at depths of 0 – 30 m in the water column of the East China Sea and were produced in all seasons. *Globigerinoides ruber* appeared to live at depths of 0 – 50 m; the season of greatest abundance was summer – autumn. Past summer and winter SSTs could be generally reconstructed from planktonic foraminiferal assemblages. Alkenone and Mg/Ca temperatures reconstructed from core-top sediments of the East China Sea are consistent with observed annual mean SSTs and summer to autumn (June – November) SSTs (JODC dataset), respectively. Core-top summer SSTs from planktonic foraminiferal assemblages represent the observed August SST, whereas winter SSTs are ~3.6°C warmer than the observed February SST. During the late Holocene, 3 kyr averaged temperatures reconstructed from the various proxies were consistent with the current observed temperatures (JODC dataset) except for winter SSTs estimated using foraminiferal assemblages. Such winter SSTs were higher than the current February SST. When 3 kyr averaged temperatures during the late Holocene were compared with temperatures during the LGM, foraminiferal assemblage based summer SSTs were warmest and Mg/Ca based temperatures were warmer than alkenone based temperatures. However, winter foraminiferal assemblage based SSTs were 2.7 – 3.7°C cooler than alkenone and Mg/Ca based temperature estimates during the late Holocene, whereas foraminiferal assemblage based

SSTs were consistent with other proxy temperatures during the LGM. Foraminiferal assemblage based winter SSTs seem to be greatly affected by the statistical technique and/or database used for calibration and estimation. Alkenone and Mg/Ca ratio based temperature estimates are not affected by the geochemical analytical method used for quantification, nor by the calibration equations chosen for calculations. Thus, alkenones and Mg/Ca ratios appear to be the most robust choices for paleothermometry in the East China Sea.



## Acknowledgements

대학원에 진학하면 작더라도 다른 과학자들에게 이야기해 줄 수 있는 새로운 사실을 밝혀보고 싶었습니다. 쉽지만은 않았던 공부 끝에 이 논문을 작성할 수 있었고, 저의 작은 꿈이 이루어진 것 같아 뿌듯합니다. 저의 목표를 달성할 수 있게 지도해주시고 이끌어주신 이경은 교수님께 매우 감사드립니다. 논문을 작성하는 것뿐만 아니라 사소한 일 처리하는 것도 꼼꼼하게 봐주신 덕분에 저는 학부를 졸업했을 때보다 여러모로 성장한 것 같습니다.

저의 논문에 많은 관심을 가져주시고 심사해주신 노일 교수님과 이호진 교수님께 감사드립니다. 그리고 전공 지식 외에도 교수님들의 경험담을 들려주시며 진심어린 조언과 격려를 해주신 해양과학기술전문대학원 교수님들께도 감사드립니다. 또 사소한 질문에도 잘 답해주고 조언을 많이 해줬던 지영언니와 용기오빠, 실험실에 처음 들어왔을 때 실험실 일을 잘 가르쳐줬던 시웅오빠와 가희언니, 실험실에서 무엇이든 항상 열심히해주는 태욱오빠, 대학원 생활을 함께 하면서 서로에게 힘이 되어줬던 나연언니, 주연언니, 효진언니에게 고맙다는 말을 전하고 싶습니다.

마지막으로 항상 저를 믿어주시고 지지해주신 부모님께 감사드리며 앞으로도 든든한 딸딸이 되겠습니다.

## References

- Anand, P., Elderfield, H. and Conte, M.H., 2003. Calibration of Mg/Ca thermometry in planktonic foraminifera from a sediment trap time series. *Paleoceanography*, 18(2), 1050. doi:10.1029/2002PA000846.
- Barker, S., Greaves, M. and Elderfield, H., 2003. A study of cleaning procedures used for foraminiferal Mg/Ca paleothermometry. *Geochemistry Geophysics Geosystems*, 4(9), 8407. doi:10.1029/2003GC000559.
- Bé, A.W.H. and Tolderlund, D.S., 1971. *Distribution and ecology of living planktonic foraminifera in surface waters of the Atlantic and Indian Oceans*. In: Funnel, B.M., Riedel, W.R. (eds) *Micropaleontology of Oceans*, 105-149. Cambridge University Press, London.
- Bijma, J., Faber, W.W. Jr. and Hemleben, C., 1990. Temperature and salinity limits for growth and survival of some planktonic foraminifers in laboratory cultures. *Journal of Foraminiferal Research*, 20(2), 95-116.
- Brassell, S.C., Eglinton, G., Marlowe, I.T., Pflaumann, U. and Sarnthein, M., 1986. Molecular stratigraphy: a new tool for climatic assessment. *Nature*, 320, 129-133.
- Chang, Y.-P., Wang, W.-L., Yokoyama, Y., Matsuzaki, H., Kawahata, H. and Chen, M.-T., 2008. Millennial-scale planktic foraminifer faunal variability in the East China Sea during the past 40000 years (IMAGES MD012404 from the Okinawa Trough). *Terr Atmos Ocean Sci*, 19(4), 389-401. doi:10.3319/TAO.2008.19.4.389(IMAGES).

- Chang, Y.-P. et al., 2009. Monsoon hydrography and productivity changes in the East China Sea during the past 100,000 years: Okinawa Trough evidence (MD012404). *Paleoceanography*, 24, PA3208. doi:10.1029/2007PA001577.
- Chen, M.-T. et al., 2005. Estimating glacial western Pacific sea-surface temperature: methodological overview and data compilation of surface sediment planktic foraminifer faunas. *Quaternary Science Reviews*, 24, 1049-1062.
- Chen, M.-T., et al., 2010. Dynamic millennial-scale climate changes in the northwestern Pacific over the past 40,000 years. *Geophysical Research Letters*, 37, L23603. doi:10.1029/2010GL045202.
- Dekens, P.S., Lea, D.W., Pak, D.K. and Spero, H.J., 2002. Core top calibration of Mg/Ca in tropical foraminifera: Refining paleotemperature estimation. *Geochemistry Geophysics Geosystems*, 3(4). doi:10.1029/2001GC000200.
- Elderfield, H. and Ganssen, G., 2000. Past temperature and  $\delta^{18}\text{O}$  of surface ocean waters inferred from foraminiferal Mg/Ca ratios. *Nature*, 405, 442-445.
- Hastings, D., Kienast, M., Steinke, S. and Whitko, A.A., 2001. A comparison of three independent paleotemperature estimates from a high resolution record of deglacial SST records in the tropical South China Sea. *Eos Trans. AGU*, 82(47), Fall Meet., Suppl., Abstract PP12B-10.
- Ijiri, A. et al., 2005. Paleoenvironmental changes in the northern area of the East China Sea during the past 42,000 years. *Palaeogeography Palaeoclimatology Palaeoecology*, 219, 239-261. doi:10.1016/j.palaeo.2004.12.028.
- Imbrie, J. and Kipp, N.G., 1971. A new micropaleontological method for quantitative paleoclimatology: application to a Late Pleistocene Caribbean core. In: Turekian KK (ed) *The Late Cenozoic Glacial Ages*, Yale University Press, New Haven, pp 71-181.

- Jian, Z. et al., 2000. Holocene variability of the Kuroshio current in the Okinawa Trough, northwestern Pacific Ocean. *Earth and Planetary Science Letters*, 184, 305-319.
- Kao, S.J. et al., 2008. Enhanced supply of fossil organic carbon to the Okinawa Trough since the last deglaciation. *Paleoceanography*, 23, PA2207. doi:10.1029/2007PA001440.
- Kim, J.-H. et al., 2008. Global sediment core-top calibration of the TEX<sub>86</sub> paleothermometer in the ocean. *Geochimica et Cosmochimica Acta*, 72, 1154-1173. doi:10.1016/j.gca.2007.12.010.
- Kim, J.-H. et al., 2010. New indices and calibrations derived from the distribution of crenarchaeal isoprenoid tetraether lipids: Implications for past sea surface temperature reconstructions. *Geochimica et Cosmochimica Acta*, 74, 4639-4654. doi:10.1016/j.gca.2010.05.027.
- Kubota, Y. et al., 2010. Variations of East Asian summer monsoon since the last deglaciation based on Mg/Ca and oxygen isotope of planktic foraminifera in the northern East China Sea. *Paleoceanography*, 25, PA4205. doi:10.1029/2009PA001891.
- Lee, K.E. and Schneider, R., 2005. Alkenone production in the upper 200 m of the Pacific Ocean. *Deep-Sea Research I*, 52, 443-456. doi:10.1016/j.dsr.2004.11.006.
- Lee, K.E., Kimoto, K. and Kim, D.H., 2010. Glacial sea surface temperature of the East Sea (Japan Sea) inferred from planktonic foraminiferal assemblage. *Geosciences Journal*, 14(2), 127-134. doi:10.1007/s12303-010-0013-5.
- Li, T. et al., 2001. Heinrich event imprints in the Okinawa Trough: evidence from oxygen isotope and planktonic foraminifera. *Palaeogeography Palaeoclimatology Palaeoecology*, 176, 133-146.

- Lin, H.-L., Wang, W.-C. and Hung, G.-W., 2004. Seasonal variation of planktonic foraminiferal isotopic composition from sediment traps in the South China Sea. *Marine Micropaleontology*, 53, 447-460. doi:10.1016/j.marmicro.2004.08.004.
- Lin, H.-L., 2014. The seasonal succession of modern planktonic foraminifera: Sediment traps observations from southwest Taiwan waters. *Continental Shelf Research*, 84, 13-22. <http://dx.doi.org/10.1016/j.csr.2014.01.020>.
- Lin, Y.-S. et al., 2006. The Holocene Pulleniatina Minimum Event revisited: Geochemical and faunal evidence from the Okinawa Trough and upper reaches of the Kuroshio current. *Marine Micropaleontology*, 59, 153-170. doi:10.1016/j.marmicro.2006.02.003.
- Machida, H., 2002. Volcanoes and tephras in the Japan area. *Global Environmental Research*, 6(2), 19-28.
- Müller, P.J. et al., 1998. Calibration of the alkenone paleotemperature index  $U^k_{37}$  based on core-tops from the eastern South Atlantic and the global ocean (60° N-60° S). *Geochimica et Cosmochimica Acta*, 62(10), 1757-1772.
- Nakanishi, T., Yamamoto, M., Tada, R. and Oda, H., 2012a. Centennial-scale winter monsoon variability in the northern East China Sea during the Holocene. *Journal of Quaternary Science*, 27(9), 956-963. doi:10.1002/jqs.2589.
- Nakanishi, T., Yamamoto, M., Irino, T. and Tada, R., 2012b. Distribution of glycerol dialkyl glycerol tetraethers, alkenones and polyunsaturated fatty acids in suspended particulate organic matter in the East China Sea. *J Oceanogr*, 68, 959-970. doi:10.1007/s10872-012-0146-4.
- Nurnberg, D., Bijma, J. and Hemleben, C., 1996. Assessing the reliability of magnesium in foraminiferal calcite as a proxy for water mass temperatures. *Geochimica et Cosmochimica Acta*, 60(5), 803-814.

- Ortiz, J.D. and Mix, A.C., 1997. Comparison of Imbire-Kipp transfer function and modern analog temperature estimates using sediment trap and core top foraminiferal faunas. *Paleoceanography*, 12, 175-190.
- Ohkouchi, N., Kawamura, K., Kawahata, H. and Okada, H., 1999. Depth ranges of alkenone production in the central Pacific Ocean. *Global Biogeochemical Cycles*, 13(2), 695-704.
- Pflaumann, U., Duprat, J., Pujol, C. and Labeyrie, L.D., 1996. SIMMAX: a modern analog technique to deduce Atlantic sea surface temperatures from planktonic foraminifera in deep-sea sediments. *Paleoceanography*, 11(1), 15-35.
- Pflaumann, U. and Jian, Z., 1999. Modern distribution patterns of planktonic foraminifera in the South China Sea and western Pacific: a new transfer technique to estimate regional sea-surface temperatures. *Marine Geology*, 156, 41-83.
- Prahl, F.G., Muehlhausen, L.A. and Zahnle, D.L., 1988. Further evaluation of long-chain alkenones as indicators of paleoceanographic conditions. *Geochimica et Cosmochimica Acta*, 52, 2303-2310.
- Prell, W.L., 1985. The stability of low-latitude sea-surface temperatures: an evaluation of the CLIMAP reconstruction with emphasis on the positive SST anomalies. United States Department of Energy, Office of Energy Research, TR025, vol. 1-2. Government Printing Office, US, pp 1-60.
- Rosell-Melé, A. et al., 2001. Precision of the current methods to measure the alkenone proxy  $U^k_{37}$  and absolute alkenone abundance in sediments: Results of an interlaboratory comparison study. *Geochemistry Geophysics Geosystems*, 2, 2000GC000141.
- Rosenthal, Y. et al., 2004. Interlaboratory comparison study of Mg/Ca and Sr/Ca measurements in planktonic foraminifera for paleoceanographic

- research. *Geochemistry Geophysics Geosystems*, 5(4), Q04D09. doi:10.1029/2003GC000650.
- Sawada, K., Handa, N. and Nakatsuka, T., 1998. Production and transport of long-chain alkenones and alkyl alkenoates in a sea water column in the northwestern Pacific off central Japan. *Marine Chemistry*, 59, 219-234.
- Schouten, S., Hopmans, E.C., Schefuß, E. and Sinninghe Damsté, J.S., 2002. Distributional variations in marine Crenarchaeotal membrane lipids: a new tool for reconstructing ancient sea water temperatures? *Earth and Planetary Science Letters*, 204, 265-274.
- Schouten, S., Hopmans, E.C. and Sinninghe Damsté, J.S., 2013. The organic geochemistry of glycerol dialkyl glycerol tetraether lipids: A review. *Organic Geochemistry*, 54, 19-61. <http://dx.doi.org/10.1016/j.orggeochem.2012.09.006>.
- Sun, Y. et al., 2005. Last deglaciation in the Okinawa Trough: Subtropical northwest Pacific link to Northern Hemisphere and tropical climate. *Paleoceanography*, 20, PA4005. doi:10.1029/2004PA001061.
- Tanaka, Y. 2003. Coccolith fluxes and species assemblages at the shelf edge and in the Okinawa Trough of the East China Sea. *Deep-Sea Research II*, 50, 503-511.
- Ternois, Y. et al., 1996. Production pattern of alkenones in the Mediterranean Sea. *Geophysical Research Letters*, 23(22), 3171-3174.
- Thompson, P.R., 1981. Planktonic foraminifera in the western north Pacific during the past 150 000 years: comparison of modern and fossil assemblages. *Palaeogeography Palaeoclimatology Palaeoecology*, 35, 241-279.
- Tierney, J.E., 2014. *Biomarker-based inferences of past climate: The TEX<sub>86</sub> Paleotemperature proxy*. In *Treatise on Geochemistry*, 2nd ed. pp. 379-393.

- van Donk, J., 1977.  $\delta^{18}O$  as a tool for micropalaeontologists. In Ramsay ATS (ed) Oceanic Micropalaeontology, ACADEMIC PRESS, London, New York, San Francisco, pp. 1345–1370.
- Waelbroeck, C. et al., 1998. Improving past sea surface temperature estimates based on planktonic fossil faunas. *Paleoceanography*, 13(3), 72–283.
- Xu, X., Yamasaki, M., Oda, M. and Honda, M.C., 2005. Comparison of seasonal flux variations of planktonic foraminifera in sediment traps on both sides of the Ryukyu Islands, Japan. *Marine Micropaleontology*, 58, 45–55. doi:10.1016/j.marmicro.2005.09.002.
- Yamamoto, M. et al., 2012. Glycerol dialkyl glycerol tetraethers and TEX<sub>86</sub> index in sinking particles in the western North Pacific. *Organic Geochemistry*, 53, 52–62. <http://dx.doi.org/10.1016/j.orggeochem.2012.04.010>.
- Yamasaki, M. and Oda, M., 2003. Sedimentation of planktonic foraminifera in the East China Sea: evidence from a sediment trap experiment. *Marine Micropaleontology*, 49, 3–20. doi:10.1016/S0377-8398(03)00024-0.
- Yu, H. et al., 2009. Variations in temperature and salinity of the surface water above the middle Okinawa Trough during the past 37 kyr. *Palaeogeography Palaeoclimatology Palaeoecology*, 281, 154–164. doi:10.1016/j.palaeo.2009.08.002.
- Zhou, H. et al., 2007. Sea surface temperature reconstruction for the middle Okinawa Trough during the last glacial-interglacial cycle using C<sub>37</sub> unsaturated alkenones. *Palaeogeography Palaeoclimatology Palaeoecology*, 246, 440–453. doi:10.1016/j.palaeo.2006.10.011.